IOPscience iopscience.iop.org

Home Search Collections Journals About Contact us My IOPscience

A parametric study of laser induced ablation–oxidation on porous silicon surfaces

This article has been downloaded from IOPscience. Please scroll down to see the full text article.

2008 J. Phys.: Condens. Matter 20 265009

(http://iopscience.iop.org/0953-8984/20/26/265009)

View the table of contents for this issue, or go to the journal homepage for more

Download details:
IP Address: 129.252.86.83
The article was downloaded on 29/05/2010 at 13:18

Please note that terms and conditions apply.

J. Phys.: Condens. Matter **20** (2008) 265009 (5pp) doi:10.1088/0953-8984/20/26/265009

A parametric study of laser induced ablation–oxidation on porous silicon surfaces

Luca De Stefano[1], Ilaria Rea[1,2], M Arcangela Nigro[1], Francesco G Della Corte[1] and Ivo Rendina[1]

[1] National Council of Research-Institute for Microelectronic and Microsystems-Department of Naples, Via P Castellino 111, 80131 Naples, Italy
[2] Department of Physics-'Federico II', University of Naples, Via Cinthia, 4-80126 Naples, Italy

E-mail: luca.destefano@na.imm.cnr.it

Received 27 March 2008, in final form 18 April 2008
Published 28 May 2008
Online at stacks.iop.org/JPhysCM/20/265009

Abstract
We have investigated the laser induced ablation–oxidation process on porous silicon layers having different porosities and thicknesses by non-destructive optical techniques. In particular, the interaction between a low power blue light laser and the porous silicon surfaces has been characterized by variable angle spectroscopic ellipsometry and Fourier transform infrared spectroscopy. The oxidation profiles etched on the porous samples can be tuned as functions of the layer porosity and laser fluence. Oxide stripes of width less than 2 μm and with thicknesses between 100 nm and 5 μm have been produced, depending on the porosity of the porous silicon, by using a 40× focusing objective.

1. Introduction

Porous silicon (PSi) is a nanostructured material fabricated by electrochemical etching of silicon in a hydrofluoric acid (HF) solution. The porosity and the thickness of a single layer are functions of the current density and of the anodization time for a fixed doping level of the silicon wafer and HF concentration. The refractive index of the PSi film depends on its porosity, and can be calculated in the frame of several effective average approximations, such as the Bruggemann or Maxwell–Garnett models [1]. Therefore, the refractive index profile of a structure can be modulated by choosing the proper current density profile and the etching time. In recent years, several PSi multilayers, such as optical waveguides [2–4], Bragg mirrors [5], micro-cavities [6] and rugate filters [7] have been investigated and proposed for specific applications as passive photonic components or sensing devices [8, 9]. Transparency in the near infrared region, room temperature photoluminescence [10], non-linear optical response [11], and high specific surface area, which assures an effective interaction with the surrounding environment, make PSi a quite ideal photonic transducer in chemical or biological monitoring. Even though the PSi fabrication compatibility with standard integrated circuit processes has been recently demonstrated, so that it could be usefully employed in so-called smart sensors [12], one of the major challenges is the integration of this technology within the micro-electro-mechanical systems. The formation of a porous area on a micro-machined silicon wafer generally requires the definition of a pre-patterned region through the standard photolithography. In this case two problems could arise: the photoresist mask is effective only for 2–3 min against the HF solution during the electrochemical process [13] and for longer etching times, a different masking material such as silicon nitride, is needed; then, the photoresist developer, being alkaline, can damage and dissolve the porous silicon. The first proposed alternative technique to the traditional photolithographic approach is direct photo-structuring of porous silicon in HF [14]. A non-wet option to the direct patterning process is laser induced ablation–oxidation. This is a powerful technique already used in direct writing of a micropattern on the PSi surface in order to define channel waveguides [15, 16] or oxidized regions for the selective cell growth [17]. Due to the low thermal conductivity of the PSi, the high temperature required for the writing process (about 900 °C) can be obtained by a low power laser [18].

 © 2008 IOP Publishing Ltd Printed in the UK

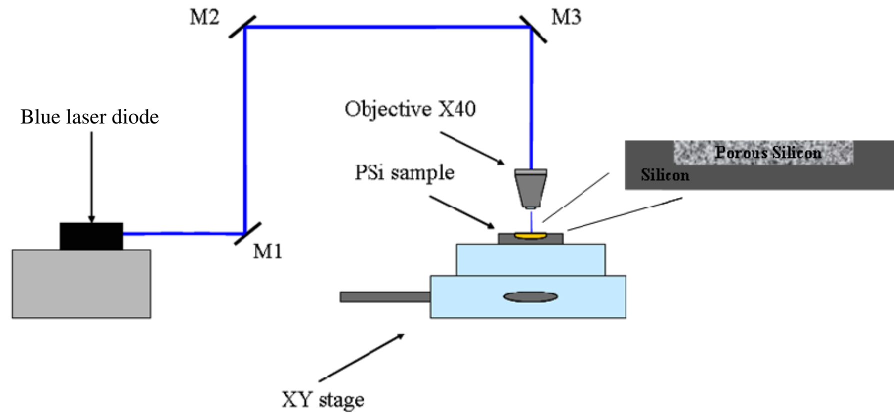

Figure 1. Scheme of the experimental setup: the blue light of a diode laser beam is shaped by a 1 mm pinhole and carried by three mirrors (M1, M2, and M3) onto the sample of PSi placed on a micrometric stage (x–y resolution 1 μm).

(This figure is in colour only in the electronic version)

Table 1. Morphological characteristics and fabrication parameters of the PSi samples.

Sample	Porosity (%)	Thickness (μm)	Anodization time (s)	Current density (mA cm^{-2})	HF concentration (50 wt%)
A	45	2	6.8	135	50
B	60	0.5	1.07	481	50
C	70	5	20.16	122	30
D	72	5	19.30	150	30
E	80	5	36.49	135	30

In this work, we have exploited—and investigated by non-destructive optical measurements—the laser induced ablation–oxidation process on several samples of PSi characterized by different porosities. The samples have been irradiated with a blue laser diode at various fluences between 38 mJ mm^{-2} and 3.8 J mm^{-2}.

2. Materials and methods

We have fabricated five PSi layers characterized by porosities in a range between 45 and 80%, while the mean pore diameter ranges from about 30 nm up to 80 nm [19]. The samples were obtained by electrochemical etching of a highly doped p$^+$-type standard silicon wafer, ⟨100⟩ oriented, 10 mΩ cm^{-1} resistivity, 400 μm thick, in a HF–C_2H_5OH solution in the dark and at room temperature. After the etching, the samples were rinsed in C_2H_5OH and dried under a stream of N_2. In table 1, we report the morphological characteristics and the fabrication parameters of the PSi samples.

The local laser ablation–oxidation of the PSi layers is a room temperature process, obtained by using the experimental setup schematized in figure 1.

The samples, placed on a motorized x–y micrometric stage (x–y resolution 1 μm; scan speed 0.001–90 mm s^{-1}), have been exposed to a laser diode beam (48 mW @406 nm, spot diameter $\approx$ 1.5 mm) at normal incidence, focused by a 40$\times$ microscope objective lens. A pinhole, 1 mm diameter, selected the centre of the laser spot. The focused beam had a quite homogeneous spot with a 1 μm diameter and a power of 38 mW just before the surface to be oxidized. Changing the scanning speed of the beam, the laser energy densities ranged between 38 mJ mm^{-2} and 3.8 J mm^{-2}.

The optical characterization of the oxidized area by variable angle spectroscopic ellipsometry (ellipsometer model UVISEL, Horiba–Jobin–Yvon) required the fabrication of an oxidized area large enough to match the size of the ellipsometer micro-spot (about 150 μm). This zone has been obtained by multiple adjacent irradiations with equal laser energy density. Ellipsometric measurements were performed at an incidence angle of 65°, in the 370–850 nm wavelength region with 1 nm spectroscopic resolution. The morphology of the PSi layers was also investigated by scanning electron microscopy (SEM) (Tescan Mira). The presence of Si–O–Si bonds due to the oxidation process has been monitored by means of infrared spectroscopy with a Fourier transform spectrometric microscope (FT-IR) (Nicolet Continuum). Spectra were obtained at a 4 cm^{-1} resolution averaging 200 scans.

On some samples, we have removed the oxidized regions by rinsing the PSi layers in a low concentration HF-based solution for 10 s. The depth of the grooves has been measured by a profilometer (KLA-TENCOR P15) with a vertical resolution of 1 nm and a horizontal resolution of 1 μm.

3. Experimental results and discussion

Even if the optical power density used in our experiment was quite high with respect to the other values reported in the literature [15, 20], we have not found any light sculpturing effect of the PSi surface for scan speed faster than 10 mm s^{-1}, corresponding to a fluence lower than 3.8 mJ mm^{-2}.

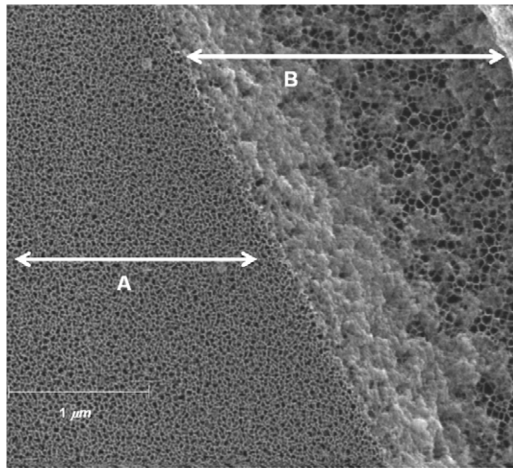

Figure 2. Scanning electron micrograph top view of the laser oxidized region on the PSi layer ($P = 72\%$): (A) almost oxidized porous silicon surface; (B) channel ablated by laser light at 3.8 J mm^{-2}.

In figure 2 the SEM top view of the laser oxidized region at 3.8 J mm^{-2} on the PSi layer with a porosity of 72% is reported. Two distinct zones are shown: the oxidized surface (A) can be easily recognized by the presence of very small pores, due to volume expansion accompanying the oxidation process. The oxide nature of this surface is also confirmed by backscattered electron images (data not shown here). The second one (B) is an ablated strip, 2 μm broad and approximately 0.5 μm deep, observed in the superficial area where the temperature profile, induced by the beam shape, exceeds the melting point of the PSi. The presence of this ablation has been also revealed by profilometric measurements. In this region the vertical distribution of the silicon oxide down to the first porous silicon layer is visible too. The asymmetry of the laser induced effect in the (A) and (B) zones can be attributed to a slight distortion of the beam profile and, consequently, to the asymmetric temperature distribution on the PSi surface.

Ellipsometric measurements confirm the bulk structuring of the PSi surface after the ablation–oxidation treatment. To fit the ellipsometric data, we have used a three EMA (effective medium approximation) layer model since the porosity of the PSi structure decreases towards the Si-substrate [21]. Figure 3 shows the three-layer model for the sample before (a) and after (b) the local ablation–oxidation together with the reflectivity spectra of both samples (c); the thickness (in nm) and the material content (%) of each layer are reported with the respective errors (in brackets) calculated by fitting the experimental data of the ellipsometric measurements. Before the oxidation, each EMA layer consists of silicon and void; the total thickness of the structure is approximately 5 μm. After the oxidation, the sample's silicon is almost completely replaced by SiO_2 (figure 3(b)), and the porosity is reduced on average to approximately 50%.

The thermal oxide, due to the local irradiation by high optical density, not only grows in the silicon nanocrystals, but also in the pores with a volume ratio 2:1, so that the smaller pores can be completely filled by the oxide, resulting in a homogeneous silica layer as evidenced by the ellipsometric results of figure 3(b).

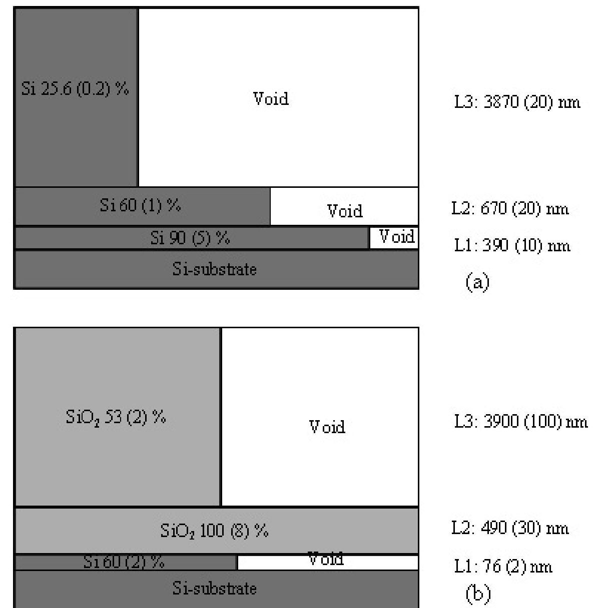

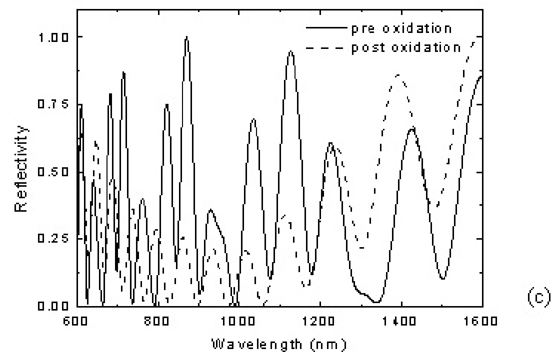

Figure 3. The three-layer model used in the ellipsometric analysis of the PSi sample ($P = 72\%$) before (a) and after (b) the local laser oxidation; (c) the reflectivity spectra of the two samples calculated from ellipsometric measurements.

The reflectivity spectrum is calculated from the measurements of the standard ellipsometric parameters [22], the irradiated sample (dashed curve in figure 3(c)) is blue shifted with respect to the fresh sample (continuous curve in figure 3(c)): the optical path (nd, where n is the refractive index and d the layer thickness) in the fresh sample is approximately 8455 nm, while it is approximately 5687 nm in the irradiated sample. As soon as the superficial layer is irradiated, it becomes transparent to the laser light, thus avoiding any further heating so that the process is self-stopping. This effect is due to the very low thermal conductivity of the porous silica and also to the high reflectivity interface at the boundary between the porous silica and the porous silicon which causes the line width to be weakly dependent on the laser fluence, while it strongly depends on the layer porosity.

The oxide growth has also been monitored by FT-IR measurements. The FT-IR spectra of the PSi layer, before and after the laser irradiations, at two different energy densities, are shown in figure 4. We have verified, as already reported

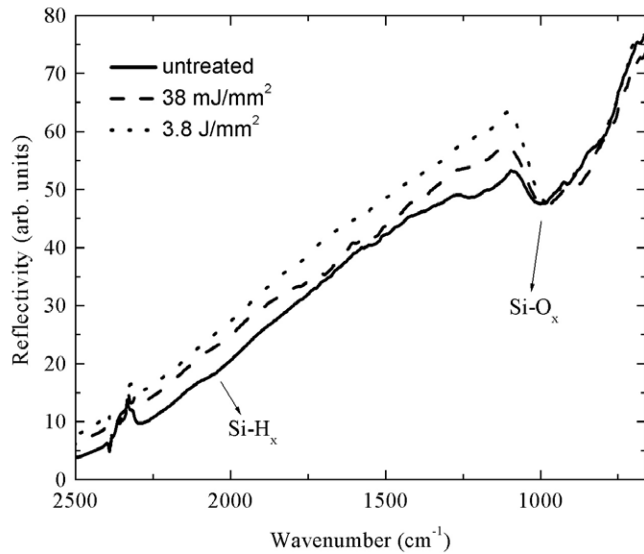

Figure 4. FT-IR spectra of the PSi layer ($P = 72\%$) before (solid line) and after laser irradiation with 38 mJ mm^{-2} (dashed line) and 3.8 J mm^{-2} (dotted line).

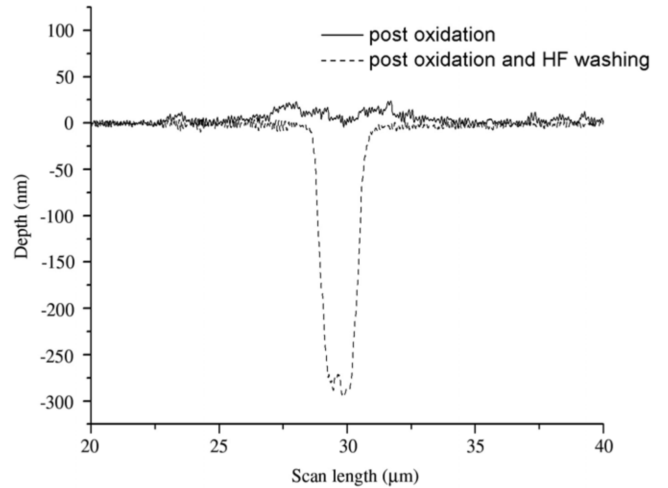

Figure 5. Profilometer analysis of the oxidized strip on the 60% porosity sample before (solid line) and post (dashed line) the HF removal.

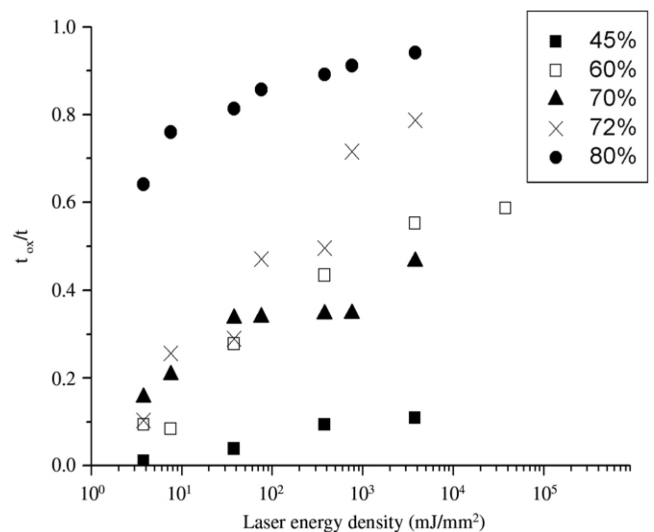

Figure 6. Ratio between the oxidized depth t_{ox} and the PSi thickness t versus the laser fluence for different starting porosities.

by Rocchia and co-workers [23], the decreasing of the Si-H$_x$ band's intensity (at 2100 cm^{-1}) and the presence of stronger Si-O$_x$ peaks (1000–1100 cm^{-1}) in the PSi FT-IR spectra by increasing the laser energy densities. This effect has been measured by calculating the peak area of the silicon oxide grown on the surface of the sample with 72% porosity at different laser fluences. In the case of PSi as-etched, we have obtained a value of 3800 counts cm^{-1}, after irradiation by an energy density of 38 mJ mm^{-2} the peak area becomes 4200 counts cm^{-1}, and for a 3.8 J mm^{-2} laser fluence we have measured 5300 counts cm^{-1}, thus confirming the expansion of the oxide in the PSi layer as the delivered light energy increases. In figure 5, we have reported the vertical profile of the oxidized strip obtained on the 60% porosity sample with a fluence of 3.8 J mm^{-2} before (solid line) and after (dash line) HF removal. Before the HF washing, the strip shows an irregular shape: a 4 nm large groove is confined between two margins approximately 20 nm high, due to the mechanical and thermal strain, as observed in previous works about the laser oxidation of silicon on insulator [24, 25]. After the HF rinsing, the local oxide is completely removed, and a 3 μm large and 280 nm deep V groove appears. By repeating this measurement on the other samples, we have found that the oxidation depth t_{ox} increases with the porosity and the absorbed laser energy densities. In particular, for the lowest porosities (45 and 60%) t_{ox} shows a rapid saturation with the laser fluence, reaching 0.3 μm for the deepest strip obtained. In this regime of porosity, there is probably competition between thermal oxidation and photo-oxidation. The behaviour is different for the higher porosities, where t_{ox} continuously increases within the explored laser fluence range. Figure 6 shows the ratio between the oxidation depth t_{ox} and the total film thickness t. The rate of this process increases with the porosity, so that the sample at 80% porosity is almost totally oxidized at the average energy density used.

The penetration of the laser light into the PSi bulk is favoured in high porosity structures. This is also confirmed by the value of $1/\alpha$ which is the light penetration depth, estimated by the ellipsometer measurement at 406 nm on the fresh material. The $1/\alpha$ coefficient value increases with the porosity: we have calculated a value of 200 nm for the sample at 45%, while the layer with 72% porosity is characterized by a penetration depth of 2400 nm. The strong dependence of the laser induced ablation–oxidation at higher values of porosity suggests a thermal nature of this phenomenon rather than a pure photo-induced one. Another key factor is the oxygen penetration which is completely inhibited by the presence of the oxidized layer where pores have been filled by the oxide expansion.

An important issue of a patterning process is represented by its repeatability: we have experimentally verified that for a given sample porosity and a fixed laser power the grooves

obtained are perfectly identical, so that it is possible to predict the oxidation depth in the device design phase. Nevertheless, some substantial differences can arise if the process is used on aged samples: the spontaneous oxidation of the porous silicon surface makes the laser oxidation less effective and the geometrical features of the grooves could be different even on the same surface if light was etched on different days. There is also a good repeatability in twin samples on the condition that they are processed on the same day.

4. Conclusions

We have studied by different analytical techniques the effect of a low power laser on a PSi layer as a function of its porosity. By using a 406 nm wavelength laser diode, we found that, for a porosity as low as 60%, only thin PSi films ($<$300 nm) can be efficiently oxidized by the laser light. Deeper oxidized porous layers can be obtained when the porosity increases, since the absorption coefficient increases too. We have demonstrated that the direct writing of oxidized stripes is approximately twice the laser beam area and up to 5 μm thick on silicon surfaces having different porosity. The laser oxidation is characterized by a slight ablation of the PSi surface, due to the high temperature induced by the light and the very low thermal coefficient of the porous material. We have also shown that two fast and non-destructive optical techniques, such as variable angle spectroscopic ellipsometry and Fourier transform infrared spectroscopy, can quantitatively control the optical structuring of the porous silicon surface. We believe that our calibration of the laser direct writing could allow an easy way to realize simple geometries on porous silicon surfaces, avoiding complex photolithography processes.

References

[1] Hardeman R W, Beale M I J, Gasson D B, Keen J M, Pickering C and Robbins D J 1985 *Surf. Sci.* **152/153** 1051
[2] Arrand H F, Benson T M, Loni A, Arens-Fischer R, Kruger M, Thonissen M, Luth H and Kershaw S 1998 *IEEE Photon. Technol. Lett.* **10** 1467
[3] Nagata S, Matsushita S, Saito K, Ohshita Y, Maeda Y, Ymaguci M and Ikushima A J 2003 *Appl. Phys. Lett.* **82** 2559
[4] Pirasteh P, Charrier J, Dumeige Y, Haesaert S and Joubert P 2007 *J. Appl. Phys.* **101** 083110
[5] Snow P A, Squire E K, Russell P S J and Canham L T 1999 *J. Appl. Phys.* **86** 1781
[6] Mulloni V and Pavesi L 2000 *Appl. Phys. Lett.* **76** 2523
[7] Lorenzo E, Oton C J, Capuj N E, Ghulinyan M, Navarro-Urrios D, Gaburro Z and Pavesi L 2005 *Appl. Opt.* **44** 5415
[8] De Stefano L, Rendina I, Moretti L and Rossi A M 2003 *Mater. Sci. Eng.* B **100** 271
[9] Ouyang H, Striemer C and Fauchet P M 2006 *Appl. Phys.* **88** 163108
[10] Canham L T 1990 *Appl. Phys. Lett.* **57** 1046
[11] Chen R, Lin D L and Mendoza B 1993 *Phys. Rev.* B **48** 11879
[12] Barillaro G, Bruschi P, Pieri F and Strambini L M 2007 *Phys. Status Solidi* a **204** 1423
[13] Tao Y and Esashi M 2004 *J. Micromech. Microeng.* **14** 1411
[14] Lerondel G, Romestain R, Vial J C and Thonissen M 1997 *Appl. Phys. Lett.* **71** 196
[15] Rossi A M, Amato G, Camarchia V, Boarino L and Borini S 2001 *Appl. Phys. Lett.* **78** 3003
[16] Rossi A M, Borini S, Boarino L and Amato G 2003 *Phys. Status Solidi* a **197** 284
[17] Khung Y, Graney S D and Voelcker N H 2006 *Biotechnol. Prog.* **22** 1388
[18] De Stefano L, Rendina I, Moretti L, Rossi A M and Tundo S 2004 *Appl. Opt.* **43** 167
[19] Timoshenko V Y, Dittrich T, Sieber I, Rappich J, Kamenev B V and Kashkarov P K 2000 *Phys. Status Solidi* a **182** 325
[20] Juan M, Bouillard J S, Plan J, Bachelot R, Adam P M, Lerondel G and Royer P 2007 *Phys. Status Solidi* a **204** 1276
[21] Wongmanerod C, Zangooie S and Arwin H 2001 *Appl. Surf. Sci.* **172** 117
[22] Azzam R M A and Bashara N M 1986 *Ellipsometry and Polarized Light* 1st edn (Amsterdam: Elsevier Science)
[23] Rocchia M, Rossi A M, Boarino L and Amato G 2005 *Phys. Status Solidi* a **202** 1658
[24] Deutschmann R A, Huber M, Neumann R, Brunner K and Abstreiter G 1999 *Micro. Eng.* **48** 367
[25] Micheli F and Boyd I W 1987 *Appl. Phys. Lett.* **51** 1149